

# Glass Transition Temperatures In Binary Polymer Blends

IOANNIS M. KALOGERAS,<sup>1</sup> WITOLD BROSTOW<sup>2</sup>

<sup>1</sup>Solid State Physics Section, Department of Physics, University of Athens, Panepistimiopolis, Zografos 157 84, Greece

<sup>2</sup>Laboratory of Advanced Polymers and Optimized Materials (LAPOM), Department of Materials Science and Engineering and Department of Physics, University of North Texas, Denton, Texas 76203-5310

Received 22 July 2008; revised 1 October 2008; accepted 3 October 2008

DOI: 10.1002/polb.21616

Published online in Wiley InterScience (www.interscience.wiley.com).

**ABSTRACT:** Knowledge of the glass transition temperatures ( $T_g$ s) as function of composition reflects miscibility (or lack of it) and is decisive for virtually all properties of polymer-based materials. In this article, we analyze single blend-average and effective  $T_g$ s of miscible polymer blends in full concentration ranges. Shortcomings of the extant equations are discussed to support the need for an alternative. Focusing on the deviation from a linear relationship, defined as  $\Delta T_g = T_g - \varphi_1 T_{g,1} - \varphi_2 T_{g,2}$  (where  $\varphi_i$  and  $T_{g,i}$  are, respectively, the weight fraction and the  $T_g$  of the  $i$ -th component), a recently proposed equation for the blend  $T_g$  as a function of composition is tested extensively. This equation is simple; a quadratic polynomial centered around  $2\varphi_1 - 1 = 0$  is defined to represent deviations from linearity, and up to three parameters are used. The number of parameters needed to describe the experimental data, along with their magnitude and sign, provide a measure of the system complexity. For most binary polymer systems tested, the results obtained with the new equation are better than those attained from existing  $T_g$  equations. The key parameter of the equation  $a_0$  is related to parameters commonly used to represent intersegmental interactions and miscibility in binary polymer blends. © 2008 Wiley Periodicals, Inc. *J Polym Sci Part B: Polym Phys* 47: 80–95, 2008

**Keywords:** blends; differential scanning calorimetry (DSC); glass transition; glass transition temperature; intermolecular interactions; polymer blends; polymer miscibility

## SCOPE

The glass transition is an important phenomenon that characterizes a range of amorphous systems, including homopolymers, polymer blends, copolymers, and polymer networks. The related experimental signals and the underlying process on a molecular scale involve both kinetic and thermo-

dynamic features.<sup>1,2</sup> For example, the influence of the direction of the change (freezing a liquid, melting a solid) and of variations in the change rate (heating or cooling) on the location of the glass transition region are illustrative of its kinetic character, whereas the experimental observation of features attributed to a second order transition is in line with the thermodynamic character.<sup>2</sup>

Although the change from the glassy state into either a liquid or a rubbery state is a gradual one, and thus the glass transition phenomenon spans a wide temperature window, experimentalists

Correspondence to: I. M. Kalogeras (E-mail: ikaloger@phys.uoa.gr)

*Journal of Polymer Science: Part B: Polymer Physics*, Vol. 47, 80–95 (2009)  
© 2008 Wiley Periodicals, Inc.

tend to report and tabulate unique values of the so-called glass transition temperature ( $T_g$ ), by analogy with the melting temperature  $T_m$  values, so as to represent a glass transition region by a single number. This permits determination of the use and processing temperature for many materials, and easier comparisons between systems of different composition and/or architecture. Different techniques lead to different  $T_g$  values.<sup>3</sup>  $T_g$  evaluations based on common thermal analysis techniques, such as differential scanning calorimetry (DSC), dynamic mechanical analysis (DMA), dielectric analysis (DEA), and thermomechanical analysis, are in general not identical. This is related to different natures and time responses of the experimental probes (motions of side- or main-chain polar groups, or of small or large parts of the chain; electrical, mechanical or thermal stimulation of the motion, etc). There are also differences of compatibility in the effective volume size averaged by each technique.<sup>2</sup> Even when one uses DEA only, the results are not necessarily the same when one obtains a  $T_g$  value from dielectric relaxation spectroscopy [e.g., from isochronal permittivity  $\epsilon'(T)$  plots or the peak of the segmental mode observed in dielectric loss  $\epsilon''(T)$ , electric loss modulus  $M''(T)$  or  $\tan \delta = \epsilon''/\epsilon'$  plots] or using thermally stimulated current spectroscopy (e.g., from the temperature at which the  $\alpha$ -relaxation band reaches a maximum in current density versus  $T$  plots).<sup>4</sup>

Although these complications exist,  $T_g$  values are useful indeed for a variety of purposes. Particularly needed are  $T_g$  values as a function of composition  $\phi$  for binary polymer blends; they tell us whether the blends are miscible, semimiscible (called compatible) or not miscible at all. As a rule of thumb, observation of a single (usually broad) glass transition region (i.e., a single  $T_g$ , the “blend-average”  $T_g$ ) for all the blends is used for establishing full miscibility (one-phase mixture). Nevertheless, this statement is an oversimplification of the actual picture. A number of miscible polymer mixtures—particularly blends whose components show a strong difference in their  $T_g$ 's and weak intermolecular interactions—present strong asymmetry. Motions of the different chains are decoupled and the relaxation dynamics of each component are clearly discernible. Along these lines, two glass transition regions have recently been distinguished in some systems,<sup>5</sup> either by means of carefully performed DSC experiments<sup>6–9</sup> or by using techniques of increased resolving power (DEA,<sup>6,10,11</sup> temperature-modu-

lated DSC (TMDSC),<sup>12</sup> DMA,<sup>6</sup> nuclear magnetic resonance,<sup>13</sup> electron spin resonance,<sup>14</sup> quasi-elastic neutron scattering,<sup>15</sup> etc). The aforementioned findings should not be confused with the case of compatibility, in which any experimental technique detects two  $T_g$  values that also depend on composition. Immiscible polymers (not an infrequent case) clearly demonstrate two  $T_g$  values for the respective pure components that are independent of composition. In each of the aforementioned cases components' miscibility (or lack of it) is decisive for all properties of the blends.

Apart from miscibility, the  $T_g$ s reflect also many features and properties of polymeric systems: helical twisting power in chiral nematic phases; changes of  $T_g$  with residual stress; effects of fillers, polymer intercalation or clay exfoliation on thermal properties; perturbations of the segmental dynamics resulting from polymer's confinement in ultrathin films or nanopore environments; consequences of aging, adsorption of solvents or hydration processes, and so forth. When we wish to achieve compatibility, then changes in  $T_g$  represent a measure of success of that operation and thus allow optimization of curing conditions or of the compatibilizing agent concentration.

The aforementioned arguments corroborate the ongoing efforts to predict the compositional dependence of various thermophysical properties, of  $T_g$  in particular, of polymer-based materials. In the following section we discuss shortcomings of the existing approaches. We thus demonstrate the need for an analytical equation for  $T_g$  as a function of concentration that will not be subjected to model-specific limitations and also could serve for blends as well as for copolymers with varying concentrations of the constituents.

## EARLIER $T_g$ VERSUS COMPOSITION EQUATIONS

Several approaches based on kinetic or thermodynamic features of the glass transition phenomenon have been proposed to provide a theoretic foundation for the equations currently used to predict -and subsequently explain- the compositional dependence of the  $T_g$  of blends of miscible polymers as well as those of random copolymers.<sup>16–24</sup> In the case of binary polymer blends, most of the derived equations are based on the assumption of additivity for the respective basic

properties of the blend components, that is, either of the specific volumes as Gordon and Taylor have proposed,<sup>23</sup> which is practically equivalent to the additivity of the relevant free volumes, as Kovacs has shown,<sup>17</sup> or of the flexible bonds contributing to the conformational changes, as DiMarzio has suggested.<sup>25</sup> These additivity models lead to the Gordon-Taylor (GT) equation<sup>23</sup>

$$T_g = \frac{\varphi_1 T_{g,1} + k_{GT}(1 - \varphi_1) T_{g,2}}{\varphi_1 + k_{GT}(1 - \varphi_1)} \quad (1)$$

for the compositional dependence of the  $T_g$  in a binary (1 + 2) polymer blend. Here,  $\varphi_i$  are the mass (weight) fractions ( $\varphi_2 = 1 - \varphi_1$ ) and  $T_{g,i}$  are the  $T_g$ s of the blend components, with the subscript two referring to the component with the higher  $T_g$ . The above equation is apparently based on the concept that one of the components has a lesser effect on the  $T_g$  of the blend than the other. The model specific parameter  $k_{GT}$ , which has to be evaluated from the experimental data, represents the unequal contributions. In the case of the common volume-additivity approach (a free volume model)  $k_{GT}$  equals  $(\rho_1/\rho_2)(\Delta\alpha_2/\Delta\alpha_1)$ , where  $\rho_i$  are the densities and  $\Delta\alpha_i = (\alpha_{\text{melt}} - \alpha_{\text{glass}})_i$  are increments at  $T_g$  of the isobaric expansivities of the blend components. Assuming the validity of the empirical Simha-Boyer rule,<sup>26</sup>  $\Delta\alpha T_g = 0.133$  (constant), and neglecting in a first approximation the influence of the densities of the blend components (i.e., assuming that  $\rho_1 \approx \rho_2$ ), the specific  $k_{GT}$  parameter for volume additivity can also be substituted by the respective reversed ratio of the  $T_g$ s of the blend components, that is,  $k_{GT} \approx T_{g,1}/T_{g,2}$ . This transforms eq 1 to the well-known Fox equation<sup>22</sup>

$$\frac{1}{T_g} = \frac{\varphi_1}{T_{g,1}} + \frac{1 - \varphi_1}{T_{g,2}} \quad (2)$$

The Fox equation assumes random mixing between the two components, equal values of the heat capacity jump in the glass transition region between the two components (i.e.,  $\Delta C_{p,1} = \Delta C_{p,2}$ ), and volume of mixing  $V^E = 0$  in the entire concentration range. Equation 2 allows prediction of blend properties from properties of pure components only and for that reason is one of the most frequently used relations. However, eq 2 falls short in describing the experimentally observed positive or negative deviations of the blend  $T_g$  from the predicted additivity values and clearly fails to describe experimental data showing complex (nonmonotonic, e.g., s-shaped) compositional

dependences. Similarly, the GT expression explains only monotonous deviations from additivity, either negative ( $0 < k_{GT} < 1$ ) or positive ( $k_{GT} > 1$ ) ones.

To account for the effect on  $T_g$  of intercomponent interactions in the liquid and glassy state of polymer mixtures, empirical concentration second-order power equations have been proposed in the literature. Jenckel and Heusch,<sup>21</sup> for instance, suggested for plasticized polymer blends the expression

$$T_g = \varphi_1 T_{g,1} + (1 - \varphi_1) T_{g,2} + b(T_{g,2} - T_{g,1})\varphi_1(1 - \varphi_1) \quad (3)$$

with  $b$  a parameter that characterizes the solvent quality of the plasticizer. To account for specific interaction, which may perturb the free volume additivity in the polymer mixture, Kwei<sup>24</sup> extended the GT equation to a concentration second-order power equation of the form

$$T_g = \frac{\varphi_1 T_{g,1} + k_{Kw}(1 - \varphi_1) T_{g,2}}{\varphi_1 + k_{Kw}(1 - \varphi_1)} + q\varphi_1(1 - \varphi_1) \quad (4)$$

by introducing in eq 1 a quadratic term,  $q\varphi_1(1 - \varphi_1)$ , with  $q$  in the role of an interaction-dependent parameter. The  $k_{Kw}$  parameter is also treated as a real fitting parameter to be evaluated from the experimental data. When  $k_{Kw} = 1$ , the Kwei equation reduces to the Jenckel-Heusch equation with  $b = q/(T_{g,2} - T_{g,1})$ . S-shaped curves can then be explained, but only with positive deviations from additivity in the low- $T_g$  range and negative deviations in the high- $T_g$  range. To reproduce negative deviations in the low- $T_g$  range and positive deviations in the high- $T_g$  range, additional correction terms have to be used.

Several other concentration second-order power equations for the compositional dependence of the blend transition temperature can be found. For example, DiMarzio<sup>25</sup> presented an equation considering the concept of flexible bond additivity along with effects of volume changes due to the different specific volumes of the blend components at  $T_g$ . Kanig<sup>27</sup> related changes in interaction energies to the respective Gibbs functions of generating one mole of holes in the equilibrium polymer melt. Nevertheless, each of the above equations can only describe the behavior of a narrow range of systems and thus the quest for alternatives remains open. Brekner and coworkers<sup>28</sup> put forward a virial-like concentration third-order equation to account for the dependence of blend  $T_g$  from the free volume distribution and the related

conformational mobility, which is controlled by the probability of hetero-molecular contact formation in the mixture due to specific interactions of the components including the energetic effects induced by conformational changes. This leads to the Brekner-Schneider-Cantow relation

$$T_g = T_{g,1} + (T_{g,2} - T_{g,1})[(1 + K_1)(1 - \varphi_1) - (K_1 + K_2)(1 - \varphi_1)^2 + K_2(1 - \varphi_1)^3] \quad (5)$$

where both  $K_1$  and  $K_2$  are obtained by fitting to experimental  $T_g$  versus concentration data.

## DEVELOPMENT OF A NEW EQUATION

Typically, the description of the  $T_g$  of miscible blends involves the use of functions that are linear in concentration [e.g., eq 1] and correspond to the first factor of a series expansion, as well as functions with higher terms that involve quadratic [e.g., eqs 3 and 4] and cubic terms of the blend composition.<sup>16,28</sup> Let us consider here another approach: In the simplest possible case, the glass transition of a miscible binary polymer blend will be a linear function of composition:  $T_g = \varphi_1 T_{g,1} + (1 - \varphi_1) T_{g,2}$ . Such an equation would have the advantage of the Fox equation (eq 2), namely predictability in terms of properties of pure components only. However, the literature data for polymer systems, involving either amorphous + amorphous polymer or amorphous + semicrystalline polymer blends, or even mixtures between two semicrystalline polymers that are miscible in the amorphous state, usually demonstrate considerable deviations from linearity. We quantify this situation by  $\Delta T_g$

$$\Delta T_g = T_g - T_g^{\text{lin}} = T_g - [\varphi_1 T_{g,1} + (1 - \varphi_1) T_{g,2}] \quad (6a)$$

The shape of the resultant deviation versus composition plot should depend on characteristics of the specific pair of polymers (e.g., molecular weight, tacticity, chemical groups, and specific interactions), with possible contributions from a number of factors, which include special material preparation procedures (use of solvents, irradiation, etc). Let us consider another relatively simple (but not rare) case:  $\Delta T_g \neq 0$  but can be represented by a parabola, that is,  $\Delta T_g = \varphi_1(1 - \varphi_1)a_0$ , where  $a_0$  is a semiquantitative measure of the deviation observed in a given system.  $\Delta T_g$  will now have the highest value at  $\varphi_1 = \varphi_2 = 0.5$ . At

that point we have  $\varphi_1 - \varphi_2 = 2\varphi_1 - 1 = 0$ . Bearing in mind the fact that real systems usually demonstrate more complicated behavior, the  $\Delta T_g(\varphi_1)$  graph is likely to show a more or less asymmetric shape. To account for such cases, let us define a quadratic polynomial centered around  $2\varphi_1 - 1 = 0$  to represent deviations from linearity:

$$\Delta T_g = \varphi_1(1 - \varphi_1) [a_0 + a_1(2\varphi_1 - 1) + a_2(2\varphi_1 - 1)^2] \quad (6b)$$

Combining eq 6a,b we obtain:

$$T_g = \varphi_1 T_{g,1} + (1 - \varphi_1) T_{g,2} + \varphi_1(1 - \varphi_1) [a_0 + a_1(2\varphi_1 - 1) + a_2(2\varphi_1 - 1)^2] \quad (7)$$

The last term in eq 7 encompasses contributions from several factors that influence the thermal characteristics of miscible binary polymer blends, including variations in the strength of the intermolecular interactions, irregular free-volume modifications, and different types of segregation of the amorphous fractions with respect to the crystalline phase.

The proposed equation contains three adjustable parameters,<sup>29</sup> their significance is explored below using a large number of examples (see ‘‘Calculations and Confrontation with Experiment’’ section). The experimental data analyzed here have been obtained using conventional DSC. However, our approach is clearly applicable also to  $T_g(\varphi)$  diagrams obtained by other techniques.<sup>4</sup>

## SYSTEMS INVESTIGATED

Published DSC data for a large number of miscible binary polymer blends were examined here (Table 1), covering a wide range of weight-average molecular weights ( $M_w$ ), blends of different state (with completely amorphous components, one or even two semicrystalline components), and blends with a wide range of differences in the  $T_g$ s of their components ( $T_{g,2} - T_{g,1}$  between 8 and 248 K). Unless otherwise stated, the single  $T_g$  values presented in Table 1 and those used in the following calculations (see ‘‘Calculations and Confrontation with Experiment’’ section), correspond to the so-called ‘‘blend-average’’  $T_g$ , that is, the single  $T_g$  value obtained from the midpoint of the heat capacity change in second-heating DSC scans. For a number of polymer blends considered here

**Table 1.** Mixture Information and Curve-Fitting Results for the Parameters Incorporated in Eq 7<sup>a</sup>

Binary Polymer Blend (1 + 2)	$\bar{M}_{w,1}$ (g/mol)	State	$\bar{M}_{w,2}$ (g/mol)	State	$\Delta T_g$ (K)	Fitting Parameters			Ref.
						$a_0$	$a_1$	$a_2$	
Linear variation of blend $T_g$									
PECH + PHB	700,000	Amorphous	150,000	Semicryst.	24	$-3.2 \pm 0.8$	0	0	0.9988 [30]
PTA + PVME	4000	Semicryst. ( $\phi_1 > 0.8$ )	64,000	Amorphous	41	$-2.1 \pm 0.7$	0	0	0.9991 [31]
Negative deviations from additivity rule									
PMMA + PaMSAN	14,000	Amorphous	96,500	Amorphous	26	$-6.3 \pm 0.4$	$3 \pm 1$	0	0.9999 [32]
PTT + PET		Semicryst.		Semicryst.	28	$-7.9 \pm 0.6$	0	0	0.9985 [33]
PC + Polyester	28,100	Amorphous	65,700	Amorphous	48	$-25.7 \pm 1.2$	$-5 \pm 1$	0	0.9999 [34]
PVE + PI	60,200		11,500		68	$-54 \pm 2$	0	0	0.9980 [35]
PVAc + PMMA	260,000		198,000	Amorphous	73	$-38 \pm 1$	$26 \pm 2$	0	0.9999 [36]
PS + PPE	144,000	Amorphous	1500	Amorphous	24	$-25 \pm 2$	0	0	0.9996 [37]
			3100		76	$-17 \pm 1$	$10 \pm 2$	0	0.9998
			5900		97	$-25 \pm 3$	0	0	0.9998
			44,000		122	$-25 \pm 1$	0	0	0.9990
PS + PPO	97,200	Amorphous	69,000	Amorphous	118	$-45 \pm 2$	0	0	0.9680 [38]
PVME + PS	21,900	Amorphous	69,800	Amorphous	129	$-142 \pm 8$	$33 \pm 24$	0	0.9903 [10]
PVME + P2CS	96,000	Amorphous	450,000	Amorphous	154	$-150 \pm 8$	$81 \pm 28$	0	0.9977 [39]
PVME + PoClIS	52,000	Amorphous	69,500	Amorphous	154	$-185 \pm 5$	$46 \pm 8$	0	0.9985 [12]
PCL + SAN	40,400	Semicryst. ( $\phi_1 > 0.5$ )	169,000	Amorphous	160	$-130 \pm 17$	0	0	0.9892 [40]
PCL + P4HSBR	80,000	Semicryst. ( $\phi_1 > 0.5$ )		Amorphous	213	$-224 \pm 4$	$95 \pm 12$	0	0.9989 [41]
PCL + TMPC	40,400	Semicryst. ( $\phi_1 > 0.5$ )	40,000	Amorphous	250	$-153 \pm 5$	$67 \pm 15$	0	0.9996 [40]
Positive deviations from additivity rule									
PaMS + PCHMA	1500		3400		8	$19 \pm 1$	$-14 \pm 2$	$-30 \pm 5$	0.9949 [42]
PMMA + CAP	100,000	Amorphous	70,000	Amorphous	50	$9 \pm 1$	$8 \pm 2$	0	0.9998 [43]
PEI (Uitem 1000) + Celanese PBI		Amorphous		Amorphous	208	$127 \pm 16$	$-58 \pm 45$	0	0.9840 [44]
Irregular deviations from additivity rule									
PMMA + PVPh	66,000	Amorphous	21,000	Amorphous	66	$2.3 \pm 3.2$	$55 \pm 6$	$46 \pm 6$	0.9990 [45]
PEO + CAB	17,350	Semicryst. ( $\phi_1 \geq 0.4$ )	25,300	Amorphous	148	$-268 \pm 22$	$-79 \pm 54$	$443 \pm 119$	0.9810 [46]
PVME + PVPh	56,400	Amorphous	30,000	Amorphous	178	$-23 \pm 2$	$-107 \pm 4$	$-56 \pm 10$	0.9998 [47]
PCL + PC	23,700	Semicryst.	23,100	Semicryst.	210	$-335 \pm 14$	$65 \pm 30$	$403 \pm 76$	0.9941 [48]

<sup>a</sup> The weight fraction of the semicrystalline component in a blend, above which its partial crystallization appears, is indicated.

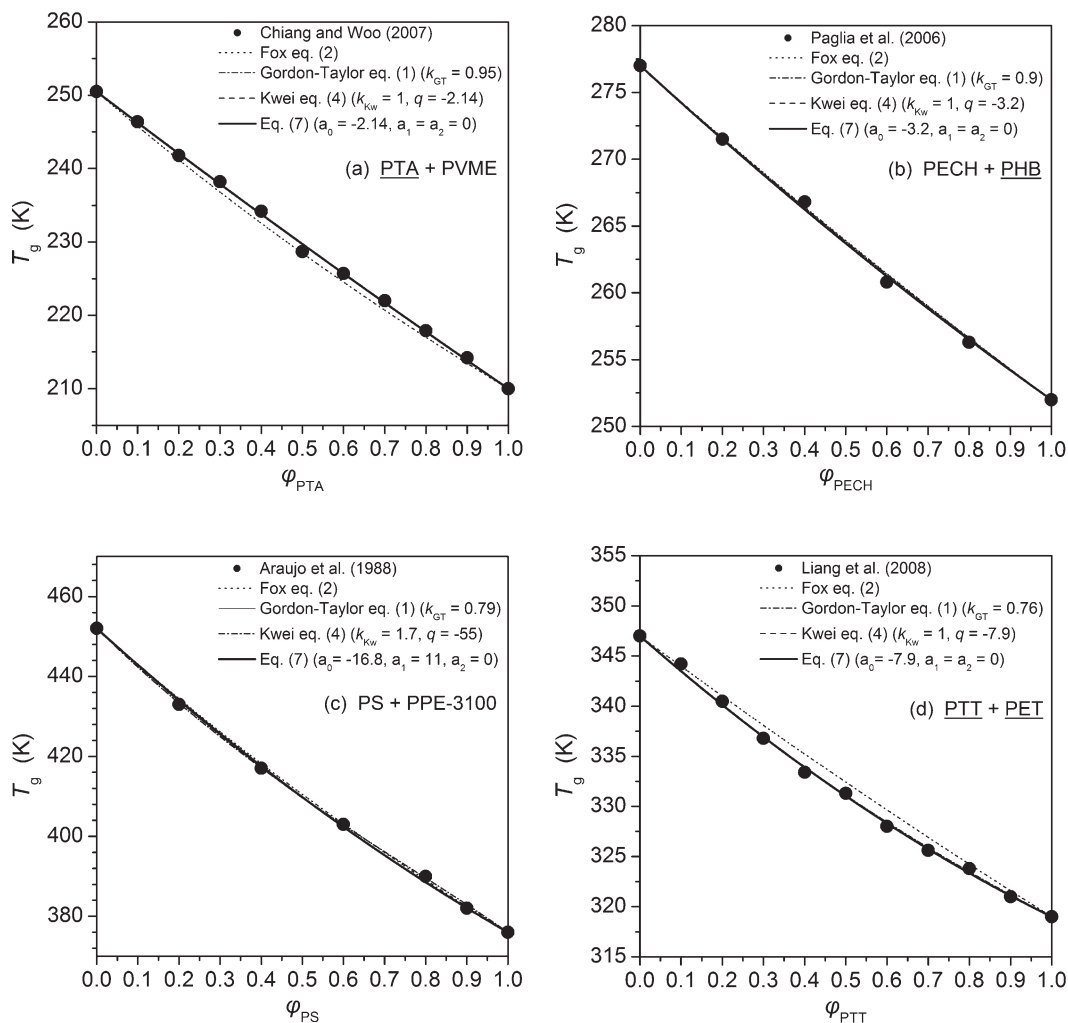


**Figure 1.** Compositional variation of blend  $T_g$  for miscible binary polymer mixtures, which obey or are very close to the ideal mass-additivity behavior (PTA + PVME and PECH + PHB) and blends that exhibit departure from it (PS + PPE-3100 and PTT + PET).

bimodal glass transition regions have been also reported; for example, in poly(vinyl methyl ether) (PVME) + polystyrene (PS),<sup>10–12</sup> poly(*n*-butyl acrylate) + PS,<sup>12</sup> PVME + poly(*o*-chloro styrene) (PoClS),<sup>12</sup> polyethylene oxide (PEO) + poly(methyl methacrylate) (PMMA),<sup>7,9</sup> PEO + poly(vinyl acetate) (PVAc),<sup>9</sup> poly(vinyl ethylene) (PVE) + polyisoprene (PI)<sup>8</sup> and poly( $\epsilon$ -caprolactone) (PCL) + PC.<sup>6</sup> For such blends, when available, analysis of DSC blend-average  $T_g$ s has been performed. We also report in “Analysis of Miscible Blends with Two  $T_g$ s” section the use of eq 7 in the case of two  $T_g$ s and discuss there the Lodge-McLeish (LM) model.<sup>5</sup> Information on the experimental details and any special procedures used for preparation of the mixtures (temperature of mixing, type

of solvent, drying processes, etc) can be found in the original references. The values reported were obtained by applying a Levenberg-Marquardt least-square minimization routine to DSC data.

## CALCULATIONS AND CONFRONTATION WITH EXPERIMENT

### Mixtures with Nearly Linear Compositional Variation of Blend $T_g$

The poly(1,3-trimethylene adipate) + poly(vinyl methyl ether) (PTA + PVME) mixture provides an example of the class of binary polymer blends which comply with the mass-additivity rule [ $\Delta T_g = 0$ , Fig. 1(a)]. Such a simple behavior is rather

rare, most likely to appear in amorphous + amorphous polymer mixtures with a low  $T_g$  difference of their pure components ( $T_{g,2} - T_{g,1} < 50$  K) and insignificant differences in the strength and level of intersegment interactions before and after mixing. One could expect large departures from this behavior to appear in blends of polymers with large contrast in their segmental mobilities and in the presence of at least one semicrystalline component. Nevertheless, the DSC data for PTA + PVME clearly demonstrate that the presence of a crystalline polyester fraction in blends with very high PTA content (for  $\phi_{PTA} > 0.8$ ) is insufficient to create even the slightest departure from linearity. Apparently, the organization of a small weight fraction of PTA in crystalline microphases has little, if any, influence on the relaxational dynamics of the chains located in the mixed amorphous phase. A similar behavior is observed in the poly(epichlorohydrin) + poly(D(-)-3-hydroxybutyrate) (PECH + PHB) blend, in which optical data reveal that after crystallization the PECH chains are rejected in the interlamellar or interfibrillar regions of PHB spherulites, where they form a homogeneous mixture with uncrystallized PHB molecules.<sup>30</sup> The completely weight-averaged behavior of the blend  $T_g$ s is described by a  $k_{GT}$  parameter nearly equal to one,  $k_{KW} = 1$  and  $q = 0$  as far as the Kwei equation is concerned, and zero values for all the parameters appearing in our equation. A small departure from the aforementioned predictions is reasonable, considering the typical experimental errors of the  $T_g$  values imposed by the resolving ability of each measuring technique (DSC, DEA, DMA,  $p$ - $V$ - $T$  data, etc). By comparing the behavior (Fig. 1) exhibited by the miscible, in the amorphous state, mixtures of PTA + PVME,<sup>31</sup> PECH + PHB,<sup>30</sup> PS + poly(2,6-dimethylphenylene ether) (PS + PPE)<sup>37</sup>, and poly(trimethylene terephthalate) + poly(ethylene terephthalate) (PTT + PET),<sup>33</sup> we expect that in the case of mass-additivity the parameters of eq 7 should obey the relations:  $|a_0| < \sim 5$ , and  $a_1, a_2 \approx 0$ . In view of that, only the first two of the systems included in Figure 1 are considered to abide by the mass-additivity rule.

### Mixtures with $\Delta T_g < 0$

A behavior of moderate complexity may be considered that of the miscible polymer systems that exhibit monotonic negative deviations from the predictions of the mass- and volume-additivity (Fox) rules. This behavior is quite common and appears

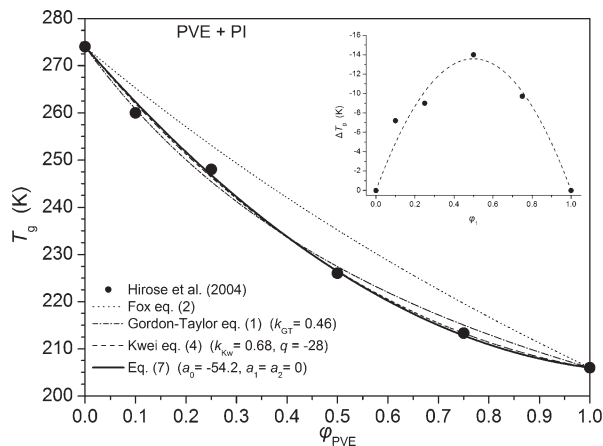


**Figure 2.** Compositional variation of blend  $T_g$  for the miscible polymer blend PVE + PI. The deviation from linearity plot is shown in the insert.

irrespective of the presence or not of a semicrystalline component in the binary polymer mixture. It characterizes blends with prevailing conformational entropic effects, which usually demonstrate a weakening of the interactions between chain segments of the stiffer component  $T_{g,2}$  due to the effect of the relatively more flexible chains of the low- $T_g$  component  $T_{g,1}$ . Representative members of this category of miscible binary mixtures are the following blends: PEO + PMMA,<sup>49,34</sup> PVAc + PMMA,<sup>36</sup> PMMA + poly( $\alpha$ -methyl styrene-co-acrylonitrile),<sup>32</sup> PS + PPE,<sup>37</sup> PS + poly(2,6-dimethylphenylene oxide),<sup>38</sup> PTT + PET,<sup>33</sup> PCL + poly(vinyl chloride) (PVC),<sup>50</sup> PCL + poly(styrene-co-acrylonitrile),<sup>40</sup> PCL + tetramethyl bisphenol-A polycarbonate (TMPC),<sup>40</sup> PVE + PI,<sup>35</sup> PVME + PS,<sup>10,12,51</sup> PVME + poly(2-chlorostyrene) (P2CS),<sup>39</sup> PVME + poly(4-hydroxystyrene) brominated (P4HSBR),<sup>41</sup> and PVAc + P4HSBR.<sup>41</sup> Experimental data for the compositional variation of the  $T_g$ s of the aforementioned systems were analyzed with use of the proposed equation and the values for the fitting parameters ( $a_0$ ,  $a_1$ , and  $a_2$ ) were compared with the parameters of the GT and Kwei equations. For this collection of miscible blends, the principal parameter in our equation ( $a_0$ ) is always negative and parameter  $a_2$  always equals zero. On the other hand, parameter  $a_1$  has been determined to be either positive (e.g., in PVME + P2CS, PVME + PS, and PCL + TMPC), zero (e.g., in PVE + PI, PS + PPE, and PEO + PMMA; see Fig. 2), or negative (e.g., in PCL + chlorinated PVC), depending on physicochemical aspects of the blend components. As expected, the

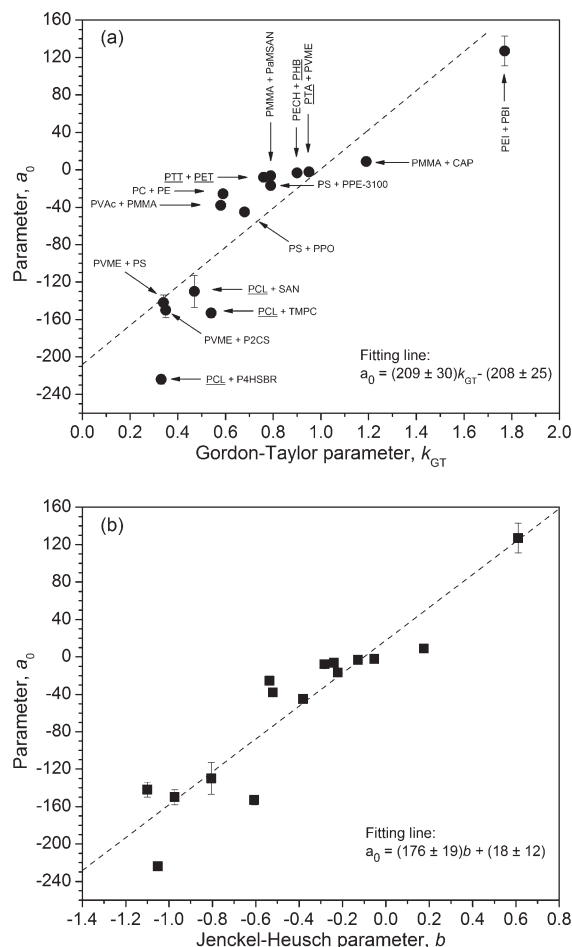


**Figure 3.** Linear fitting of the dependence between the principal parameter of the proposed equation,  $a_0$ , and the parameters of (a) the Gordon-Taylor,  $k_{GT}$ , or (b) the Jenckel-Heusch equation,  $b$  [ $b = a_0/(T_{g,2} - T_{g,1})$ ]. The data in these plots involve miscible binary polymer blends for which parameter  $a_2$  is zero. Note that for blends with  $a_1 \neq 0$ , the ratio  $a_0/(T_{g,2} - T_{g,1})$  is also nearly equal to  $b$ . The errors in the values are comparable to the size of the symbols unless otherwise indicated.

lower the value of  $a_0$  the higher the negative deviation from linearity is.

A linear relationship between the parameters  $a_0$  and  $k_{GT}$ , valued for miscible blends with  $a_2 = 0$ , appears to exist in the entire range of their variation [Fig. 3(a)], with

$$a_0 = 209k_{GT} - 208. \quad (8)$$

This dependence is in agreement with the predicted equivalence of  $a_0 = 0$  with  $k_{GT} = 1$  (mixtures with nearly linear compositional variation of blend  $T_g$ ). In the case where the experimental data fit our function with  $a_0 \neq 0$  and zero for the

higher terms, the proposed equation reduces to the Jenckel-Heusch eq 3 with  $b = a_0/(T_{g,2} - T_{g,1})$ . The data in Figure 3(b) give us a linear relation between  $b$  and  $a_0$ :

$$a_0 = 176b + 18. \quad (9)$$

Gordon and Taylor<sup>23</sup> as well as Jenckel and Heusch<sup>21</sup> claim that their equations represent intermolecular interactions. If these claims are true, so does our eq 7.

### Mixtures with Positive Deviations from the Volume- and Mass-Additivity Rules

In parallel to the aforementioned type of moderately complex blend behavior, there is a group of miscible polymer mixtures that exhibit monotonic positive deviations from the predictions of the simple mass- and volume-additivity rules for the blend  $T_g$ . These deviations are characteristic of binary blends with prevailing enthalpic effects due to strong interactions between the polymeric components. The amorphous blends of aromatic polyetherimide + polybenzimidazole (PEI + PBI)<sup>44</sup> and PMMA + cellulose acetate hydrogen phthalate (PMMA + CAP)<sup>43</sup> are representative members of this less-common class of blends. In the case of the miscible amorphous PEI + PBI blend [Fig. 4(a)], Fourier transform infrared (FTIR) data point to the presence of strong interactions, which primarily involve strong hydrogen-bond interactions ( $\delta H$ ) between the carbonyl groups of the imide ring and the amine group of the imidazole ring, and to a lower degree,  $\pi$ -orbital interactions between the imide and imidazole rings or charge-transfer interaction between the phthalimide and benzimidazole fused ring systems. The strongly positive value for our prime parameter  $a_0$  ( $a_0 = +127$ ) is in agreement with the, on the average, high strength of these interactions. In the case of the amorphous PMMA + CAP mixtures [Fig. 4(b)], the observed miscibility at all compositions and over a wide temperature range is considered to arise from intercomponent hydrogen bonding, among the carbonyl groups of PMMA and free hydroxyl groups of CAP. If one considers that the magnitude of the parameter  $a_0$  is a semiquantitative measure of the strength of the interactions, as is the accepted meaning of  $k_{GT}$ , then the low value of  $a_0 \approx +9$  for PMMA + CAP suggests  $\delta H$  interactions of reduced strength or significantly lower density of interacting groups compared to those for the miscible PEI + PBI blend. This

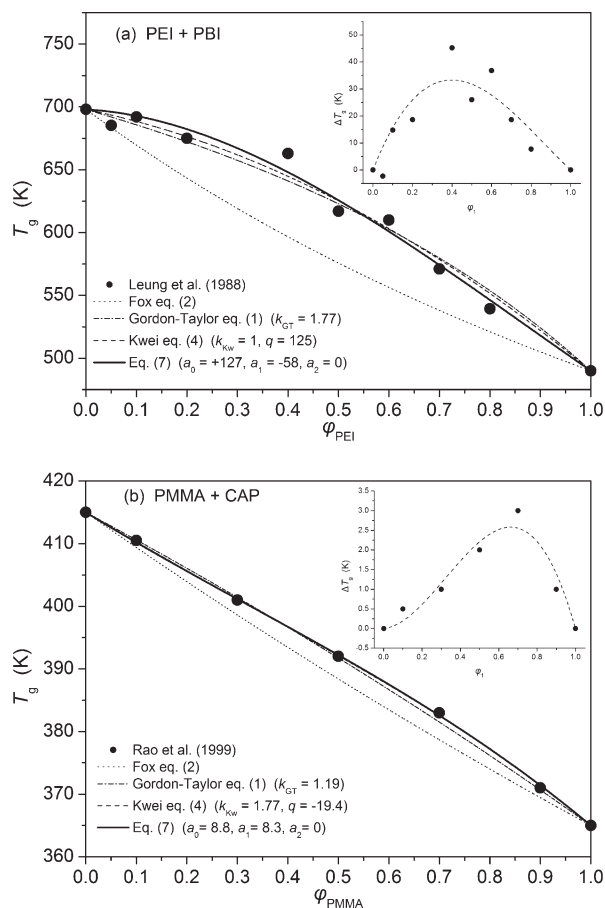


**Figure 4.** Compositional variation of blend  $T_g$  for the miscible polymer blends of (a) PEI + PBI and (b) PMMA + CAP. In each case, the deviation from linearity plot is shown in the insert.

deduction is further substantiated by the comparison of the corresponding reduced  $a_0/(T_{g,2} - T_{g,1})$  values (0.61 and 0.18, for PEI + PBI and PMMA + CAP, respectively). In both cases, however, the results obtained from the Fox equation stand apart, but we recall that these are predicted from the  $T_g$ s of pure components only - a default option if no results for blends are available. Compared to the commonly used eq 4, eq 7 is much more accurate; much lower values of the standard deviation result.

Another interesting observation for this type of behavior involves the different signs of the second significant parameter in our equation,  $a_1$ . The negative sign, namely  $a_1 = -58$  for the first miscible blend indicates an enhanced up-shift with respect to the linear mixing rule for mixtures with the low- $T_g$  component PEI as the minority component; the maximum deviation moves below  $\phi_1 = 0.5$ , see insert in Figure 4(a). On the basis of

this observation, one could suggest that the density of interacting groups and/or the strength of their interaction is more intense when a small weight fraction of the relatively flexible PEI chains is added to a rigid PBI matrix. The behavior is reversed in the other blend, at which  $a_1$  is around +8 [insert in Fig. 4(b)].

Parameter  $a_2$  is zero in the aforementioned examples of polymer mixtures, in agreement with the assumed moderate complexity of their behavior. Nevertheless, there exist interesting cases of “anomalous” changes in the dynamics of mixtures with components of nearly equal  $T_g$ . The intriguing behavior involves either positive<sup>42,52</sup> or negative<sup>53,54</sup> departures from the mass-additivity rule, which are accompanied by blend  $T_g$ s not intermediate to those of the blend components. In an attempt to explain this phenomenon several scenarios have been invoked; for example, either changes in volume due to blending (i.e., positive or negative excess volume), changes in the intermolecular constraints, or nonrandom mixing. No matter the cause, this anomaly produces significant positive or negative values for  $a_2$ . Characteristic examples provide the miscible blends of poly( $\alpha$ -methyl styrene) (P $\alpha$ MS) with poly(cyclohexyl methacrylate) (PCHMA)<sup>42</sup> and of PECH with PVME,<sup>52</sup> in which the  $T_g$  of some blends is above the highest neat component value ( $T_{g,2}$ ). For example, in the P $\alpha$ MS + PCHMA system (Fig. 5), the  $a_0$ ,  $b$ , and  $k_{GT}$  values strongly depart from the linear  $a_0$  versus  $k_{GT}$  and  $b$  versus  $a_0$  dependences established by the data included in Figure 3. This behavior is consonant with the distinctly nonzero value of our third parameter. Note that in this case also, the proposed equation

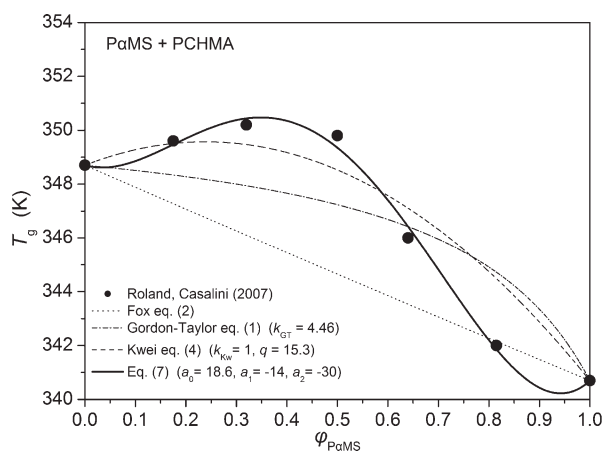


**Figure 5.** Compositional variation of  $T_g$  for the miscible polymer blends P $\alpha$ MS + PCHMA.

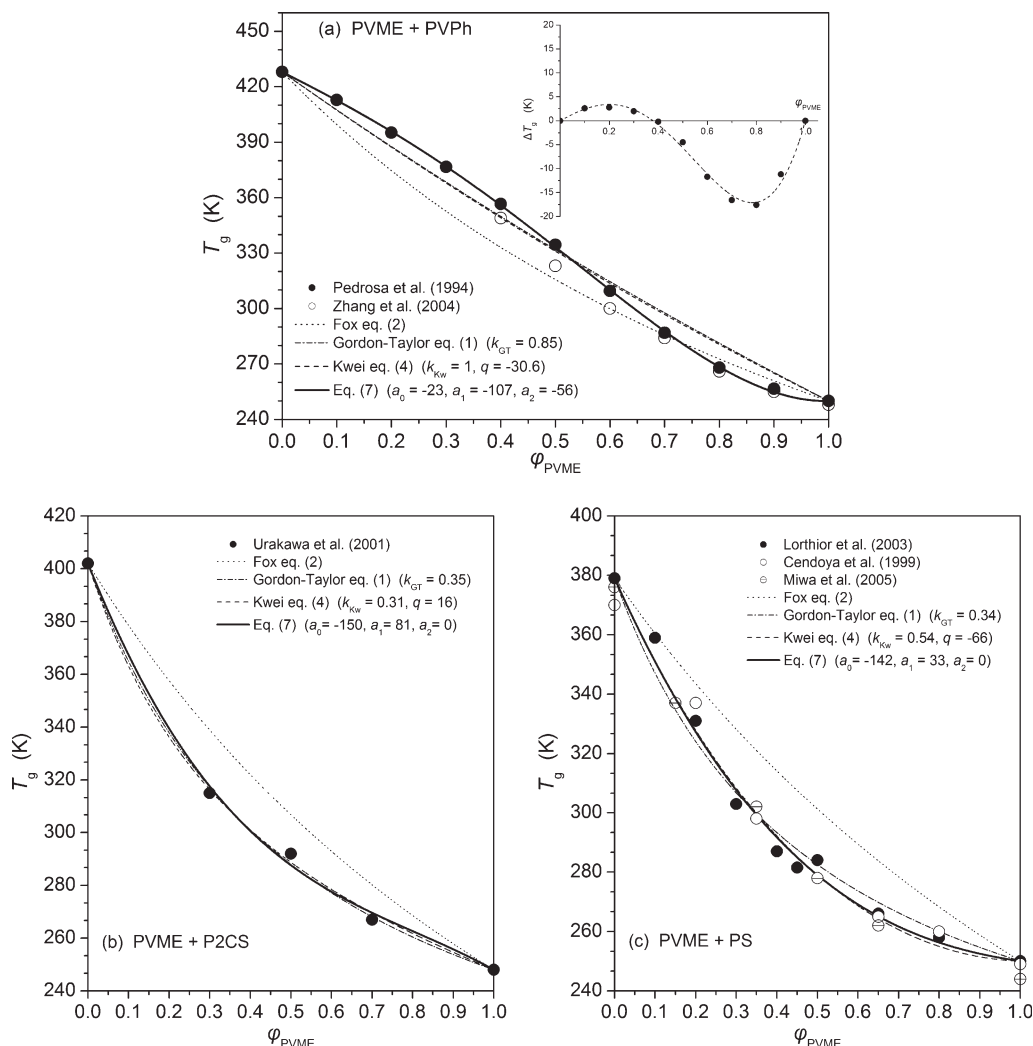


**Figure 6.** Comparison of the compositional variation of the glass transition temperatures observed in miscible blends of PVME with (a) PVPh, (b) P2CS, and (c) PS. An unusual plot (observed only in PVME + PVPh) of the  $T_g$ -deviation from the weighted-average blend  $T_g$  is shown in the insert.

provides a better fit to the experimental data -and in a wider compositional range- for the systems considered here, in comparison to the two-parameter Kwei equation or other more complex functions (e.g., see in ref. 42 the use of eq 5).

**Mixtures with Irregular Compositional Dependence of  $T_g$**

**Binary Amorphous Blends**

As already stated in “Earlier  $T_g$  Versus Composition Equations” section, the problem regarding the need to describe peculiar compositional dependences of the  $T_g$  in miscible binary blends, such as the alternating convex-concave (i.e., S-

shaped) parts in the plot, has been treated with moderate success by, among others, eq 4 of Kwei,<sup>24</sup> eq 5 of Brekner, Schneider, and Cantow,<sup>28</sup> and the model of Kovacs.<sup>17,18</sup> In general, these  $T_g$ -composition dependencies are interpreted considering mechanisms of gradual or stepwise changes in the scale of mixing for the two polymers in the blend, while the peculiar behavior is considered to indicate that the interactions and scales of mixing for the blend system are not the same and may vary with blend composition. The proposed equation succeeds to describe a wider range of anomalous behaviors of blends with high complexity. As an example, in Figure 6 we show the compositional variation of the blend  $T_g$  for miscible mixtures of amorphous PVME with poly(4-vinyl

phenol) [PVME + PVPh; Fig. 6(a), P2CS (PVME + P2CS; Fig. 6b) and PS (PVME + PS; Fig. 6(c)]. The behavior of the first system is unique for several reasons. For this system FTIR studies revealed the presence of strong intermolecular hydrogen bonds between the phenolic —OH groups in PVPh and the ether oxygen in PVME, with strength that surpasses the intrachain interactions between PVPh repeat units.<sup>55</sup> Contrary to the expected clear upshift of the blend  $T_g$ 's from the mass-mixing rule (see systems in the previous Section), the deviation of the blend  $T_g$  from linearity [insert in Fig. 6(a)] demonstrates a remarkable inversion of its sign at  $\varphi_{\text{PVME}} \approx 0.4$ . Based on the Fourier-transform infrared data of Zhang et al.<sup>55</sup> at this “critical” compositional threshold there is a change in the intercomponent coupling due to a different balancing between intermolecular and intramolecular hydrogen bonding. This modification in enthalpic characteristics of the blends is likely to induce also entropic effects that may account for the observed behavior. In another study of this polymer mixture, Pedrosa et al.<sup>47</sup> explained the peculiar shape of the  $T_g$  versus volume fraction dependence using the theory of Kovacs. The theory is based on free-volume considerations of the glass transition phenomenon, namely free-volume additivity modified for the excess volume of mixing  $V^E$ . Two different equations were used to fit the experimental data, which exhibited two well-defined regions separated by a singular point or cusp (at a critical temperature or, equivalently, a volume fraction). A linear function was used for the  $T_g$  data below the critical volume fraction of  $\varphi_c \approx 0.5$  (i.e., in PVPh-rich blends). Redrawing the  $T_g$  data of Pedrosa et al.<sup>47</sup> as function of the mass fraction of PVME [see Fig. 6(a)], the linear region transforms into a curved line with no loss of the information about the existence of a “critical” concentration.

The behavior of the two other blends stands apart; clear negative departure from the predictions of the mass- and volume-additivity rules ( $a_0 \ll 0$ ) and nonparabolic shape of the deviation from additivity plot (clearly  $a_1 > 0$ ) is observed. The former advocates for very weak intercomponent interactions and the latter indicate dissimilarity between the behaviors of blends with low and high PVME contents. We should note that the absence of strong intermolecular interactions between PVME and P2CS (or PS) and intrinsic mobility differences between the components were used by Urakawa et al.<sup>39</sup> to explain the results of their dielectric relaxation studies in

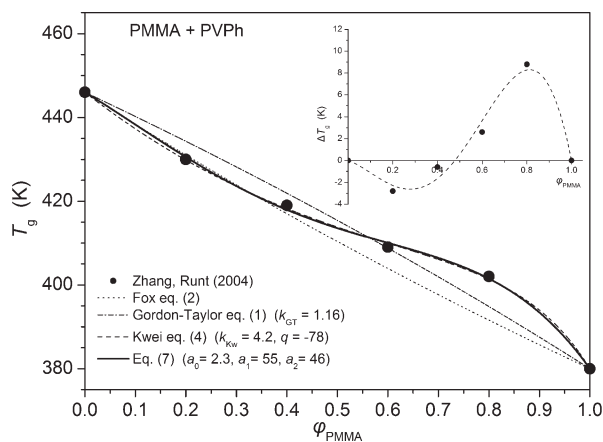


**Figure 7.** Compositional variation of blend  $T_g$  for the miscible PMMA + PVPh polymer blend. The plot of the deviation from linearity is shown in the insert.

PVME + P2CS (both components dielectrically active), which revealed that the components relax individually in their blends (i.e., two segmental relaxation dielectric modes are observed, despite the miscible state of the blends).

The blends of amorphous PMMA with PVPh (PMMA + PVPh; Fig. 7)<sup>45</sup> are another important example of complex behavior. By analogy to the deviation plot of the intermolecularly hydrogen-bonded PVME + PVPh mixture [Fig. 6(a)], the contour of the plot in this case could suggest another critical weight fraction,  $\varphi_{\text{PMMA,c}} \approx 0.5$ .

### Binary Blends with Semicrystalline Components

In the case of a crystalline-amorphous polymer pair, the miscibility is also confirmed by detection of a single  $T_g$ , which corresponds to a miscible amorphous phase formed by the amorphous fraction of the crystalline polymer and the amorphous polymer. Depression of the melting temperatures is also expected and frequently observed. Partial crystallization has considerable effect on the blend  $T_g$ , which is, however, not straightforwardly accounted for by the proposed explanations. Typically, one witness strong elevations of the experimental  $T_g$  values for blends with some amount of crystallinity in comparison to the trend followed by the completely amorphous mixtures.<sup>31,41,46,56,57</sup> The discrepancy is, to a certain extent, corrected if the experimental data are plotted not as a function of the overall weight fraction of the component in dependence of its actual weight fraction in the amorphous phase in the blend [e.g., see data for PCL + P4HSBR, Fig. 8(a)<sup>41</sup>]. One may also

observe cases where partial crystallization of one component appears at a narrow compositional window -usually, when this component is the majority phase- but the compositional variation of the blend  $T_g$  is unaltered; for example, see the

case of the PTA + PVME mixture, PTA is in a semicrystalline phase when  $\varphi_{\text{PTA}} > 0.8$ .

In contrast to the aforementioned behavior, in several cases [e.g., see Fig. 8(b,c) for PCL + PC and PEO + CAB, respectively) the peculiar non-monotonic  $T_g$  versus composition variation persists, even after the necessary corrections for the actual weight fractions of each component in the amorphous phase of the blend. In terms of microstructure such intriguing variations may be, in part, attributed to the different types of segregation of the amorphous polymer and their relative contribution in the overall structure. In order of increasing degree of segregation one finds: (a) interlamellar segregation (the amorphous polymer resides in the interlamellar region within the lamellar stack), (b) interfibrillar segregation (the amorphous chains are placed outside the lamellar stacks of the crystalline component(s), but are still located within the spherulite), and/or (c) interspherulitic segregation (the amorphous phase is expelled from the lamellar stacks and reside at the interspherulitic region). In our equation, the complexity of the system is reflected in the value of the third adjustable parameter,  $\alpha_2$ , which is found to attain remarkably high values in the case of PEO + CAB, PCL + PC, and several other mixtures of semicrystalline PC with amorphous polymers. We note that  $\alpha_2$  in eq 7 is in the present case larger by up to two orders of magnitude than in the preceding cases, demonstrating that we are dealing with more complex systems. In the case of the PCL + PC mixture, in which both components are semicrystalline, one may observe a cusp at a critical composition,  $\varphi_c$ , around 0.4, above which the Braun-Kovacs equation<sup>18</sup> can be successfully implemented (see the analysis by Cheung and Stein<sup>48</sup>). Similar arguments apply also for the PEO + CAB system. In the latter case complementary optical microscopy and small-angle X-ray scattering experiments

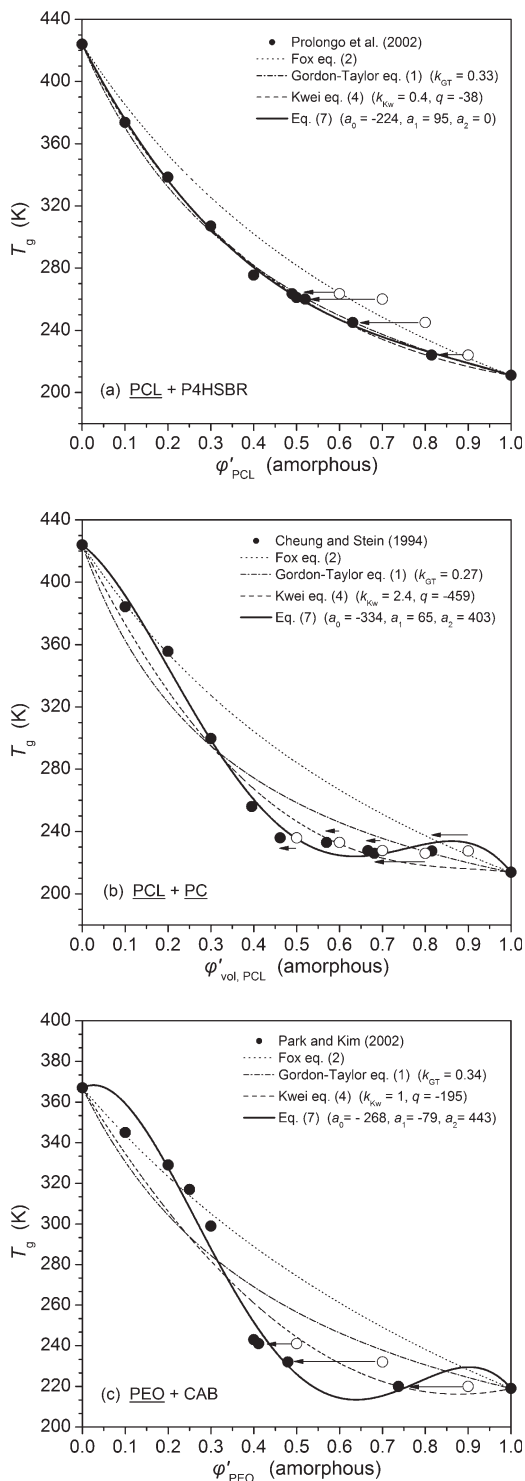


**Figure 8.** Blend  $T_g$  versus amorphous phase composition ( $\varphi'$ ) dependences reported for three miscible polymer blends with at least one semicrystalline component: (a) PCL + P4HSBR, (b) PCL + PC, and (c) PEO + CAB. Open symbols refer to the actual experimental data, plotted as function of the overall weight content of PEO in the blend ( $\varphi_1$ ), which were subsequently corrected for blend crystallinity ( $\varphi'_1 = \frac{\varphi_1 - x_{c,\text{blend}}}{1 - x_{c,\text{blend}}}$ , where  $x_{c,\text{blend}}$  is the degree of crystallinity in the blend; filled symbols denoted by arrows). For PCL + PC corrected volume fractions were used.

verified the complexity of the blend revealing that at low CAB contents the chains of the amorphous component are incorporated into interlamellar regions and commence to segregate to the interfractillar region with increase of its weight fraction.<sup>46</sup>

### Analysis of Miscible Blends with Two $T_g$ s

There are binary polymer blends presenting two concentration dependent glass transitions even when structural analysis points to a single-phase material. In such cases, thermodynamically driven concentration fluctuations, component intrinsic mobility differences, or self-concentration effects induced by chain connectivity, have been considered mainly.<sup>5,58</sup> A model developed by LM<sup>5</sup> considers self-concentration effect; because of chain connectedness the average number of nearest neighbors of a given segment which belong to the same component is larger than the number of neighboring segments of the other component. The effective local concentration  $\varphi_{\text{eff},i}$  sensed by each polymer segment is therefore represented by

$$\varphi_{\text{eff},1} = \varphi_{s,1} + (1 - \varphi_{s,1})\varphi_1 \quad (10a)$$

$$\varphi_{\text{eff},2} = \varphi_{s,2} + (1 - \varphi_{s,2})(1 - \varphi_1) \quad (10b)$$

Here,  $\varphi_{s,i}$  is the “self-concentration” of the considered polymer segment ( $i = 1, 2$ ). In the LM model, the length-scale related to the monomeric friction factor is regarded of the same order as the Kuhn length  $l_k$  defined as  $C_\infty l$ , where  $C_\infty$  is the characteristic ratio, and  $l$  is the length of the average backbone bond. One assumes that relaxation of the Kuhn segment is influenced by the concentration of segments within a volume  $V = gl_k^3$  ( $g$  is a geometric factor). Parameter  $\varphi_s$  for each blend component is calculated as the volume fraction occupied by the Kuhn length inside  $V$ :

$$\varphi_s = \frac{C_\infty M_0}{k \rho N_{\text{AV}} V} \quad (11)$$

where  $M_0$  is the molar mass of the repeat unit,  $N_{\text{AV}}$  is the Avogadro number,  $k$  is the number of backbone bonds per repeat unit, and  $\rho$  is the mass density.

Typically, the theoretic self-concentration of each component (between 0.1 and 0.6, based on calculations using eq 11) is initially used for estimating effective local concentrations (eq 10). The effective  $T_g$  of each component in the blend is

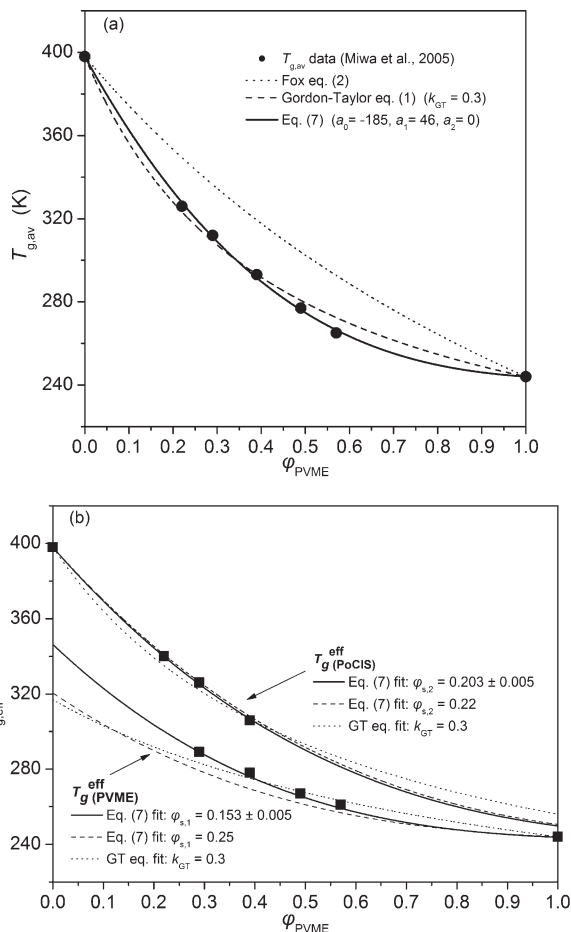


**Figure 9.** (a) Compositional variation of  $T_g$  data (●) of Miwa et al.<sup>12</sup> for PVME + PoClS blends. (b) Effective  $T_g$ s (■) of components versus  $\varphi_{\text{PVME}}$ . Explanation in text.

then evaluated using the Fox equation, with the assumption that  $T_g^{\text{eff}}(\varphi) = T_g(\varphi)|_{\varphi=\varphi_{\text{eff}}}$  and compared with the experiment (e.g.,<sup>5,6,9</sup>). Alternatively,  $\varphi_s$  can be incorporated as an adjustable parameter in eq 2; experimental  $T_g^{\text{eff}}(\varphi)$  data are now fitted to obtain  $\varphi_s$  estimates, compared then with predictions from eq 11. When the Fox equation seems unsuitable for describing the experimental  $T_{g,\text{av}}(\varphi)$  or  $T_g^{\text{eff}}(\varphi)$  dependencies, alternative fitting equations have been used such as eq 1<sup>12,14</sup> or eq 5.<sup>59</sup>

As an example of benefits of eq 7, we have applied it to a case of a miscible two- $T_g$ s system. In Figure 9(a) we show TMDSC results of Miwa et al.<sup>14</sup> for the bulk-average  $T_g$ s in PVME + PoClS blends, confronted with eqs 1, 2, and 7. Clearly our eq 7 with  $a_0 = -185$ ,  $a_1 = 46$ , and  $a_2 = 0$ , agrees with the experiment much better than the other equations. We have used  $k_{\text{GT}} = 0.3$ , reported by Miwa et al.<sup>14</sup>

**Table 2.** Comparison of the  $R^2$  Values and the Reduced  $\chi^2$ -Square  $\chi^2/\text{DoF}$  Values

Miscible Polymer System (Blend A + B)	$\Delta T_g$ (K)	Fitting Functions					
		Gordon-Taylor (Eq 1)		Kwei (Eq 4)		Equation 7	
		$\chi^2/\text{DoF}$	$R^2$	$\chi^2/\text{DoF}$	$R^2$	$\chi^2/\text{DoF}$	$R^2$
Linear compositional variation of blend $T_g$							
PECH + PHB	25	0.1144	0.9987	0.1362	0.9988	0.1089	0.9988
Negative deviations from additivity rule							
PMMA + PaMSAN	26	0.0403	0.9996	0.0254	0.9998	0.0196	0.9999
PC (Lexan) + Polyester [T(40)C-GJ]	48	0.6114	0.9984	0.2723	0.9994	0.0027	0.9999
PVE + PI	68	2.4529	0.9966	1.6541	0.9981	1.4315	0.9980
PVME + PS	129	33.83	0.9820	22.18	0.9895	20.52	0.9903
Positive deviations from additivity rule							
PzMS + PCHMA	8	3.07	0.8016	1.36	0.9266	0.118	0.9949
PMMA + CAP	50	0.317	0.9991	0.112	0.9997	0.103	0.9998
PEI + PBI	208	105.35	0.9795	92.22	0.9840	81.97	0.9840
Irregular deviations from additivity rule							
PMMA + PVPh	66	15.661	0.4571	0.457	0.9993	0.901	0.9990
PVME + PVPh	178	59.96	0.9855	63.90	0.9861	0.87	0.9998
PCL + PC <sup>b</sup>	210	324.4	0.9413	151.9	0.9752	40.9	0.9941

<sup>a</sup>The values are determined applying eqs 1, 4, and 7 to experimental data for 11 representative systems with a range of dynamic heterogeneities ( $\Delta T_g$ 's between  $\sim 10$  and 200 K).

<sup>b</sup>PHB, PCL and PC are the Semicrystalline components.

Using the aforementioned  $a_i$  values in eq 7, and substituting  $\varphi_i$  by  $\varphi_{\text{eff},i}$ , we have calculated the blend effective  $T_g$ s of each component [ $T_{g,\text{PVME}}^{\text{eff}}(\varphi)$  and  $T_{g,\text{PoClS}}^{\text{eff}}(\varphi)$ ] and the corresponding self-concentrations. In Figure 9(b) we show as solid curves the results of using eq 7 with the same  $a_0$  and  $a_1$  values as in Figure 9(a) and  $\varphi_s$  as fitting parameters. We include in Figure 9(b) predictions from eq 7 using the  $\varphi_s$  estimates of Miwa et al.<sup>12</sup> (dashed curves) and also GT (eq 1) fits reported by these authors (dotted lines). Figure 9(b) illustrates the success of our equation also in such a case.

In the LM model, the lower  $T_g$  component typically has a smaller persistence length, which leads to a larger self-concentration.<sup>5</sup> This condition was assumed to be obeyed in PVME + PoClS blends; hence Miwa et al.<sup>14</sup> used values of  $\varphi_{s,1} = 0.25$  taken from Lodge and Mc Leish<sup>5</sup> and  $\varphi_{s,2} = 0.22$  taken from Leroy et al.<sup>59</sup> for PVME and PoClS, respectively, assuming  $g = 1$ . Our eq 7 reveals a reverse trend;  $\varphi_{s,1} = 0.153 \pm 0.005$ ,  $\varphi_{s,2} = 0.203 \pm 0.005$ , with  $\varphi_{s,1}/\varphi_{s,2} = 0.75$ . Ample experimental evidence suggests that  $\varphi_s$  is matrix-dependent and corrections for the geometric factor are required.<sup>9,60,61</sup> In our analysis the geometric factor for PVME is  $g_1 = 1.634$  and  $g_2 = 0.957$  for

PoClS; the correction for the low- $T_g$  blend component is too high to be ignored. Even within the assumptions of the LM model, a length scale is of the order of Kuhn length but not necessarily equal to that length. Further support for the validity of the observed inequality ( $\varphi_{s,1}/\varphi_{s,2} < 1$ ) is provided by recent results for PCL + PC (Herrera et al.<sup>6</sup>  $\varphi_{s,1}/\varphi_{s,2} = 0.41$ ) and PEO + PMMA (Lodge et al.<sup>7</sup>  $\varphi_{s,1}/\varphi_{s,2} = 0.92$ ). In particular, Herrera et al.<sup>6</sup> analyzed their dielectric  $T_g$  results using a similar procedure and eq 5. This resulted in a better fit than given by eq 2, yielding  $\varphi_{s,1} = 0.20$  for PCL and  $\varphi_{s,2} = 0.49$  for PC. In the frame of the LM model  $\varphi_{s,2} = 0.05$ , while  $\varphi_{s,2} = 0.49$  is needed to achieve a reasonable agreement with the experimental data, a nearly 10-fold adjustment. Similar discrepancies have been reported by Urakawa et al.<sup>61</sup> for PEO + PVAc blends. Apparently in the LM model strong intermolecular interactions are underestimated.<sup>59,61</sup>

## CONCLUDING REMARKS

One can think of a hierarchy of complexity of polymeric systems. In “well behaving” miscible binary systems the simple mass-additivity or

volume-additivity rules such as the Fox equation (eq 2) might be sufficient. With increasing system complexity, GT equation (eq 1), or Jenckel-Heusch equation (eq 3), or Kwei equation (eq 4), the free-volume approach of Kovacs, and finally our  $T_g(\varphi)$  formula (7) can be used. The last equation has been confronted with experimental data for several systems and has been found to describe well even very complicated dependences of the  $T_g$  on composition. Better fit to the experimental data is seen in Table 2 in terms of the coefficient of determination ( $R$ -square) values and the reduced  $\chi$ -square values ( $\chi^2/\text{DoF}$ ,  $\text{DoF}$  = number of the degrees of freedom) obtained using eqs 1, 4, and 7. The only possible exception can be cusp-containing systems when the Braun-Kovacs equation<sup>18</sup> serves better. Otherwise our eq 7 describes all types of behavior in miscible polymer blends regardless of their complexity. Actually, the new equation alone can provide a measure of the system complexity. The number of the  $a_i$  parameters needed to reproduce well the experimental data and the relative magnitude of each parameter serve for this purpose. In very simple systems in which  $T_{g,\text{dev}}$  can be well represented by a parabola, only one parameter  $a_0$  is sufficient.

Comparisons with eqs 3 and 4 show how our  $a_0$  provides a measure of the strength of the intercomponent interactions in miscible binary polymer blends. Equations 8 and 9 should not be surprising. As demonstrated by Flory in a long series of papers, those interactions determine the behavior of binary and other multicomponent systems.<sup>62</sup> Thus, connections between different parameters that are measures of that strength are expected. With increasing system complexity the second parameter  $a_1$  acquires higher absolute values, with sign and magnitude that may be used to predict variations in the degree of “connectivity” or the attraction between the components with changes in the blend composition. The highest complexity is reflected in high values of the third parameter  $a_2$ , which reflects the presence of interesting structural phenomena. Note that mere inspection of the chemical composition and structure of each component in the mixture does not render possible to predict which class this blend will fall to. Blending-induced changes in the macroconformation and spatial organization of the polymer chains, different, at various compositions, degrees of shielding of hydrogen-bonding active chemical groups by other chain segments, and crystallization processes that become active at narrow compositional windows and show

strongly composition-dependent kinetics, are some of the factors that preclude a straightforward categorization of the blends.

Witold Brostow acknowledges discussions with the late Paul J. Flory at Stanford on structures and thermodynamic properties of polymeric systems. A partial financial support has been provided by the Robert A. Welch Foundation, Houston (Grant B-1203).

## REFERENCES AND NOTES

- Saiter, J.-M.; Negahban, M.; dos Santos Claro, P.; Delabare, P.; Garda, M.-R. *J Mater Ed* 2008, 30, 51–95; (b) Mano, J. F. *J Mater Ed* 2003, 25, 151–164; (c) Bilyeu, B.; Brostow, W.; Menard, K. P. *J Mater Ed* 2000, 22, 107–130; (d) Privalko, V. P. *J Mater Ed* 1998, 20, 57, 373–394.
- Menczel, J. D.; Prime, R. B., Eds.; *Thermal Analysis of Polymers, Fundamentals and Applications*; Wiley: New York, 2009.
- McKenna, G. B.; Simon, S. L. In *Handbook of Thermal Analysis and Calorimetry, Applications to Polymers and Plastics*; Cheng, S. Z. D., Ed.; Elsevier: Amsterdam, 2002; Vol. 3, Chapter 2, pp 49–110.
- Vassilikou-Dova, A.; Kalogeras, I. M. *Dielectric Analysis (DEA) In Thermal Analysis of Polymers, Fundamentals and Applications*; Menczel, J. D.; Prime, R. B., Eds.; Wiley: New York, 2009; Chapter 6.
- Lodge, T. P.; McLeish, T. C. B. *Macromolecules* 2000, 33, 5278–5284.
- Herrera, D.; Zamora, J.-C.; Bello, A.; Grimau, M.; Laredo, E.; Müller, A. J.; Lodge, T. P. *Macromolecules* 2005, 38, 5109–5117.
- Lodge, T. P.; Wood, E. R.; Haley, J. C. *J Polym Sci Part B: Polym Phys* 2006, 44, 756–763.
- Sakaguchi, T.; Taniguchi, N.; Urakawa, O.; Adachi, K. *Macromolecules* 2005, 38, 422–428.
- Gaikwad, A. N.; Wood, E. R.; Ngai, T.; Lodge, T. P. *Macromolecules* 2008, 41, 2502–2508.
- Lorthioir, C.; Alegría, A.; Colmenero, J. *Phys Rev E* 2003, 68, 031805.
- Leroy, E.; Alegría, A.; Colmenero, J. *Macromolecules* 2002, 35, 5587–5590.
- Miwa, Y.; Usami, K.; Yamamoto, K.; Sakaguchi, M.; Sakai, M.; Shimada, S. *Macromolecules* 2005, 38, 2355–2361.
- Haley, C. J.; Lodge, T. P.; He, Y.; Ediger, M. D.; von Meerwall, E. D.; Mijovic, J. *Macromolecules* 2003, 36, 6142–6151.
- Miwa, Y.; Sugino, Y.; Yamamoto, K.; Tanabe, T.; Sakaguchi, M.; Sakai, M.; Shimada, S. *Macromolecules* 2004, 37, 6061–6068.
- Hoffmann, S.; Willner, L.; Richter, D.; Arbe, A.; Colmenero, J.; Farago, B. *Phys Rev Lett* 2000, 85, 772–775.

16. Schneider, H. A. *J Res Natl Inst Stand Technol* 1997, 102, 229–248.
17. Kovacs, A. J. *Adv Polym Sci* 1963, 3, 394.
18. Braun, G.; Kovacs, A. J. In *Physics of Non-Crystalline Solids*; Prim, J. A., Ed.; North-Holland: Amsterdam, 1965.
19. Utracki, L. A. *Adv Polym Technol* 1985, 5, 33–39.
20. Couchman, P. R.; Karasz, F. E. *Macromolecules* 1978, 11, 117–119.
21. Jenckel, E.; Heusch, R. *Kolloid Z* 1953, 130, 89.
22. Fox, T. G. *Bull Am Phys Soc* 1956, 1, 123.
23. Gordon, M.; Taylor, J. S. *J Appl Chem* 1952, 2, 493.
24. Kwei, T. K. *J Polym Sci Lett* 1984, 22, 307.
25. DiMarzio, E. A. *Polymer* 1990, 31, 2294–2298.
26. Simha, R.; Boyer, R. F. *J Chem Phys* 1962, 37, 1003–1007.
27. Kanig, G. *Kolloid Z Z Polym* 1963, 190, 1.
28. Brekner, M.-J.; Schneider, A.; Cantow, H.-J. *Macromol Chem* 1988, 189, 2085; (b) Brekner, M.-J.; Schneider, A.; Cantow, H.-J. *Polymer* 1988, 78, 78–85.
29. Brostow, W.; Chiu, R.; Kalogeras, I. M.; Vassilikou-Dova, A. *Mater Lett* 2008, 62, 3152–3155.
30. Dubini Paglia, E.; Beltrame, P. L.; Canetti, M.; Seves, A.; Marcadalli, B.; Martuscelli, E. *Polymer* 1993, 34, 996–1001.
31. Chiang, W.-J.; Woo, E. M. *J Polym Sci Part B: Polym Phys* 2007, 45, 2899–2911.
32. Madbouly, S. A. *Polym J* 2002, 34, 515–522.
33. Liang, H.; Xie, F.; Chen, B.; Guo, F.; Jin, Z.; Luo, F. *J Appl Polym Sci* 2008, 107, 431–437.
34. Yang, H.; Yetter, W. *Polymer* 1994, 35, 2417–2421.
35. Hirose, Y.; Urakawa, O.; Adachi, K. *J Polym Sci Part B Polym Phys* 2004, 42, 4084–4094.
36. Song, M.; Long, F. *Eur Polym Mater* 1991, 27, 983–986.
37. de Araujo, M. A.; Stadler, R.; Cantow, H. J. *Polymer* 1988, 29, 2235–2243.
38. Prest, W. N., Jr.; Porter, R. S. *J Polym Sci Part A-2: Polym Phys* 1972, 10, 1639–1655.
39. Urakawa, O.; Fuse, Y.; Hori, H.; Tran-Cong, Q.; Yano, O. *Polymer* 2001, 42, 765–773.
40. Madbouly, S. A.; Abdou, N. Y.; Mansour, A. A. *Macromol Chem Phys* 2006, 207, 978–986.
41. Prolongo, M. G.; Salom, C.; Masegosa, R. M. *Polymer* 2002, 43, 93–102.
42. Roland, C. M.; Casalini, R. *Macromolecules* 2007, 40, 3631–3639.
43. Rao, V.; Ashokan, P. V.; Shridhar, M. H. *Polymer* 1999, 40, 7167–7171.
44. Leung, L.; Williams, D. J.; Karasz, F. E.; MacKnight, W. *J Polym Bull* 1986, 16, 457–464.
45. Zhang, S.; Runt, J. *J Polym Sci Part B: Polym Phys* 2004, 42, 3405–3415.
46. Park, M. S.; Kim, J. K. *J Polym Sci Part B: Polym Phys* 2002, 40, 1673–1681.
47. Pedrosa, P.; Pomposo, J. A.; Calahorra, E.; Cortazar, M. *Macromolecules* 1994, 27, 102–109.
48. Cheung, Y. W.; Stein, R. S. *Macromolecules* 1994, 27, 2512–2519.
49. (a) Zawada, J. A.; Ylitalo, C. M.; Fuller, G. G.; Colby, R. H.; Long, T. E. *Macromolecules* 1992, 25, 2896–2902; (b) Li, X.; Hsu, S. L. *J Polym Sci Part B: Polym Phys* 1984, 22, 1331–1342.
50. Chiu, F.-C.; Min, K. *Polym Int* 2000, 49, 223–234.
51. Cendoya, I.; Alegria, A.; Alberti, J. M.; Colmenero, J.; Grimm, H.; Richter, D.; Frick, B. *Macromolecules* 1999, 32, 4065–4078.
52. Alegria, A.; Telleria, I.; Colmenero, J. *J Non-Cryst Solids* 1994, 172–174, 961–965.
53. Roland, C. M. *Macromolecules* 1995, 28, 3463–3467.
54. Casalini, R.; Santangelo, P. G.; Roland, C. M. *J Phys Chem B* 2002, 106, 11492–11494.
55. Zhang, S. H.; Jin, X.; Painter, P. C.; Runt, J. *Polymer* 2004, 45, 3933–3942.
56. Kalogeras, I. M.; Vassilikou-Dova, A.; Christakis, I.; Pietkiewicz, D.; Brostow, W. *Macromol Chem Phys* 2006, 207, 879–892.
57. Kalogeras, I. M.; Stathopoulos, A.; Vassilikou-Dova, A.; Brostow, W. *J Phys Chem B* 2007, 111, 2774–2782.
58. Kumar, S. K.; Shenogin, S.; Colby, R. H. *Macromolecules* 2007, 40, 5759–5766.
59. Leroy, E.; Alegría, A.; Colmenero, J. *Macromolecules* 2003, 36, 7280–7288.
60. Lutz, T. R.; He, Y.; Ediger, M. D.; Pitsikalis, M.; Hadjichristidis, N. *Macromolecules* 2004, 37, 6440–6448.
61. Urakawa, O.; Ujii, T.; Adachi, K. *J Non-Cryst Solids* 2006, 352, 5042–5049.
62. Flory, P. J. *Selected Works*; Stanford University Press: Stanford, 1985; Vol. 3.